
A fixed methane filter maximizes freshwater emissions under warming

In the format provided by the
authors and unedited

Supplementary Information

Table of contents

Supplementary Methods	2
Supplementary Discussion: Generality of our findings across freshwater systems	3
Supplementary Fig. 4 The degree of CH ₄ over-saturation in stream water increased along the natural warming gradient.....	7
Supplementary Table 1 Current global CH ₄ emissions and estimated increases with 2.5°C of warming under SSP2-4.5 for either a fixed or optimum CH ₄ filter scenario.	8
Supplementary Table 2 Idealised complete mineralisation of glucose to CO ₂ and CH ₄	9
Supplementary Table 3 Hydrophysical characteristics for the streams in the five high-latitude regions.	10
Supplementary Table 4 Chemical characteristics for the streams in the five high-latitude regions.	11
Supplementary Table 5 Parameter estimates to characterize the temperature sensitivity in methane-related processes.....	12
Supplementary Table 6 Subset of sample DNA concentrations for downstream molecular work.....	15
Supplementary Table 7 Parameter estimates to evaluate changes in community diversity and community compositional changes along the natural warming gradient..	16
Supplementary Table 8 Parameter estimates to evaluate process-level CH ₄ oxidation efficiency and system-level CH ₄ filter efficiency..	20
Supplementary Table 9 Primer sets for qPCR and NGS.	22
References	24

Supplementary Methods

Nutrient analysis for total inorganic nitrogen (TIN: $\text{NO}_3^- + \text{NO}_2^- + \text{NH}_4^+$) and soluble reactive phosphorus (SRP) in stream water

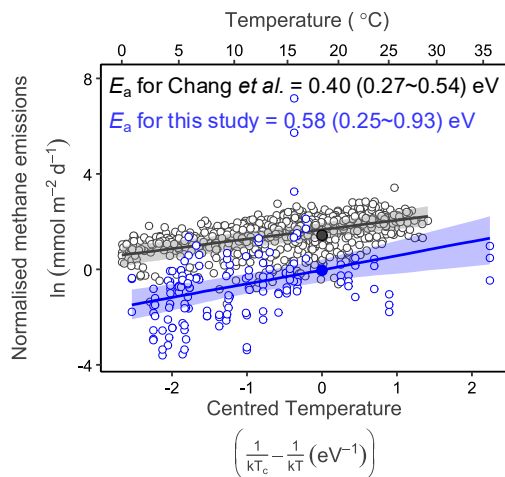
Samples of surface water (7 mL) for nutrient analyses were collected from each stream at three equally spaced locations and filtered in the field using PES Syringes fitted with 0.45 μm filters (Gilson, UK). Samples were stored in a freezer (-20°C) within 8 hours of sampling. Back at the laboratory, concentrations of nitrate (NO_3^-), nitrite (NO_2^-), ammonium (NH_4^+), and soluble reactive phosphorus (SRP) were measured colourimetrically using a segmented flow auto-analyser (Skalar, San⁺⁺, Breda, The Netherlands), according to Kirkwood (1996)¹. The limits of detection for NO_2^- , NO_x^- ($\text{NO}_2^- + \text{NO}_3^-$), NH_4^+ and SRP are 0.05 μM , 0.1 μM , 0.2 μM and 0.05 μM , respectively². The sum of NO_3^- , NO_2^- and NH_4^+ is presented as total TIN in Supplementary Table 4.

Supplementary Discussion: Generality of our findings across freshwater systems

Emissions

Because our measurements were made at a single point in the growing season, it could be argued that we missed any seasonal variation in the observed temperature – emission relationship. However, high-resolution seasonal wetland time series from Chang et al. (2021)³ show that although CH₄ flux and temperature exhibit hysteresis throughout the year, re-analysis of their dataset yields an activation energy of 0.40 eV. This value is statistically indistinguishable from the 0.58 eV we derived from our stream network spanning the Northern Hemisphere (Supplementary Fig. 1). Thus, where temporal data exist, they converge on a comparable temperature sensitivity inferred from our spatial gradients. This also agrees with our earlier meta-analysis of 127 globally distributed ecosystems⁴, based explicitly on seasonal variation in CH₄ flux and temperature. Together, these independent lines of evidence – one site-level and temporal, the other global and seasonal – demonstrate that the absence of within-stream temporal sampling in our dataset does not compromise the robustness or generality of our findings.

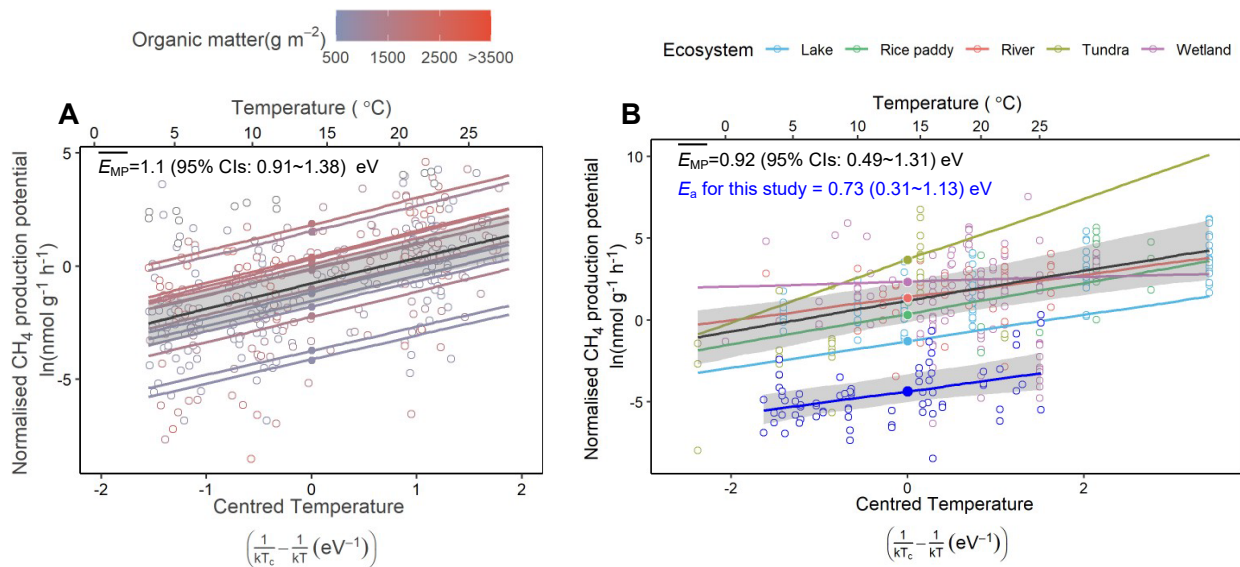
It is also notable that the absolute emission (average rate of emission at the same temperature of 18 °C, the mid-temperature of emission samples of this study, see Methods) in Chang et al.'s wetland (5.3 mmol CH₄ m⁻² d⁻¹) was ~5.5-fold higher than that from our streams (0.96 mmol CH₄ m⁻² d⁻¹). Despite these differences in each system's capacity to emit CH₄, their emissions share comparable temperature sensitivities (0.40 vs. 0.58 eV, respectively, with overlapping 95% credible intervals, Supplementary Fig. 1). This reinforces the conclusion that while absolute fluxes differ between systems, the emergent temperature sensitivity is conserved across both time and space.



Supplementary Fig. 1 | Temperature dependence of CH₄ emissions across temporal and spatial datasets. Seasonal wetland CH₄ flux data from Chang et al. (2021, blue, $n=677$ daily measurements in one wetland from 2015 to 2018)³ compared with our stream data (black, $n=148$ for 51 independent streams across 5 high latitude regions). Despite hysteresis in the seasonal record, both datasets yield statistically indistinguishable activation energies (0.40 vs. 0.58 eV, shading gives overlapping 95% credible intervals, also in parentheses). While absolute emissions differed (~5.5-fold higher in the wetland at the same 18 °C, filled circles, intercepts at T_c, 0), the emergent temperature sensitivity of emissions was conserved across temporal and spatial scales. The activation energies were quantified using hierarchical Boltzmann–Arrhenius models fit in a fully Bayesian framework as per the figures in the main text, see Methods.

Production

Similarly, because our natural experiment was based in oligotrophic, high-latitude streams with lower CH₄ production potentials than are typical for lakes, wetlands, or tundra soils, it might be expected that the temperature sensitivity may not be representative of higher CH₄ potentials. Yet in our earlier synthesis of riverine sediments, absolute CH₄ production (average rate of production at the same temperature of 14 °C, the same as the mid-temperature for measuring production in this study, see Methods) spanned more than four orders of magnitude as a function of organic matter content, but the temperature sensitivity remained conserved⁵ (Supplementary Fig. 2A). Extending this analysis to other ecosystems⁶ revealed the same pattern: lakes, wetlands, tundra soils, and rice paddies differ greatly in absolute potential rates but share a common temperature sensitivity (Supplementary Fig. 2B). Importantly, even though the CH₄ production potentials for our new high-latitude stream data were the lowest (blue, 2B), they fall directly on this cross-system relationship, demonstrating that even where absolute rates vary by >10,000-fold, the emergent temperature sensitivity of CH₄ production is robust across ecosystems.

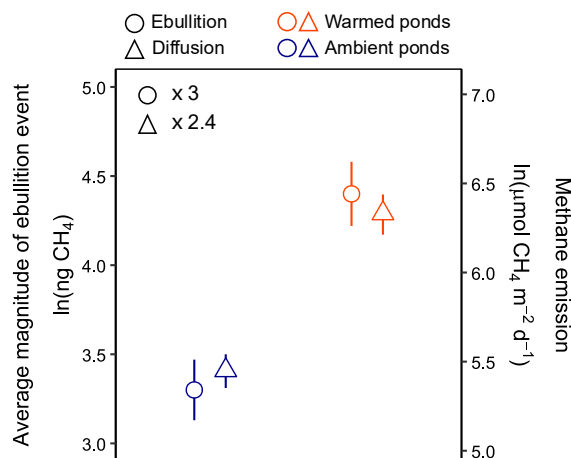


Supplementary Fig. 2 | Temperature sensitivity of CH₄ production across carbon gradients and ecosystem types. **A**, Stream sediment CH₄ production rates related to sediment organic matter content, showing >10,000-fold variation in absolute production rates (filled circles, intercepts at T_c , 0) but a conserved temperature sensitivity (1.1 eV). **B**, CH₄ production across five freshwater ecosystem types (lakes, rice paddies, rivers, tundra soils, wetlands) also revealed large differences in absolute production rates (filled circles, intercepts at T_c , 0) but a common temperature sensitivity (0.92 eV, shading gives 95% credible intervals, also in parentheses). Our high-latitude stream data (0.73 eV) overlay directly on this cross-system relationship. Data in A ($n=371$ observations across 14 independent streams) and B ($n=336$ observations across 5 ecosystem types from 32 studies) were published earlier^{5,6} but, for consistency, the activation energies were derived again here using hierarchical Boltzmann–Arrhenius models fitted in a fully Bayesian framework (as per the figures in the main text, and see Methods).

Ebullition

Ebullition has the potential to bypass the CH₄ filter and could therefore undermine the broader applicability of our conclusions. In our high-latitude streams, porewater CH₄ was too low (nM vs. mM typically required) to drive ebullition as we have shown before⁷. In systems where

ebullition is high, such as silty riverbed sediments, ebullition is known to scale with CH₄ concentration, diffusive fluxes and temperature⁸. Our own experimental warming⁹ also confirmed this proportionality (Supplementary Fig. 3). Thus, although ebullition may contribute a substantial share of emissions in some settings, the fraction of total CH₄ production oxidised before emission — i.e. system-level filter efficiency — is still expected to be conserved.



Supplementary Fig. 3 | Proportional response of diffusive and ebullitive CH₄ emissions to experimental warming. Experimental +4 °C warming increased both diffusive (mean ± s.e., $n=3555$ from 7 warmed and 7 ambient ponds) and ebullitive fluxes (mean ± s.e., $n=198$ from 7 warmed and 7 ambient ponds) proportionately, confirming that even when ebullition contributes substantially to total emissions, system-level CH₄ filter efficiency remains fixed. From Zhu et al. (2020)⁹.

Oxidation and abundance

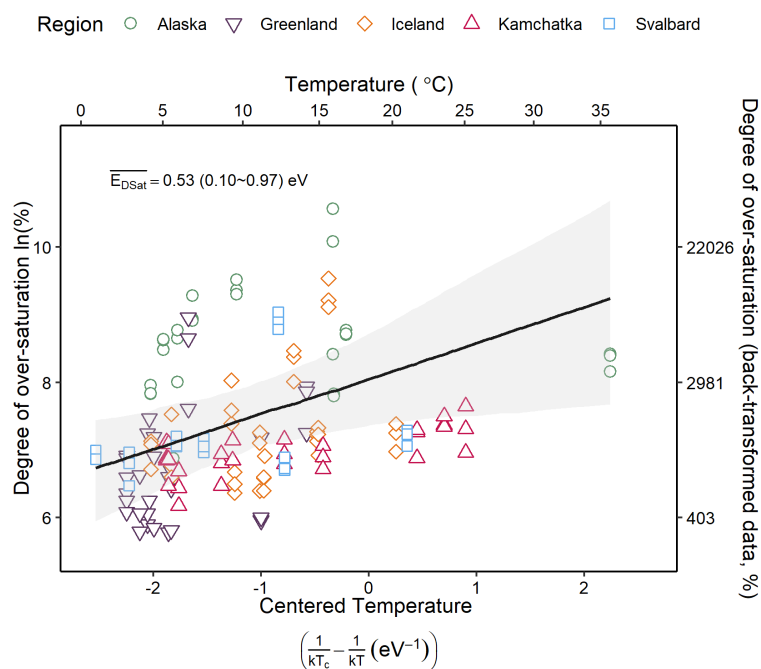
A further consideration is whether our conclusions about fixed filter efficiency can be generalised, given that comparable datasets for CH₄ oxidation and methanotroph abundance are scarce. This scarcity is precisely what makes our study novel: across five independent regions spanning the Northern Hemisphere, we consistently found that oxidation potentials increased with warming, but process-level efficiency (i.e., the turnover rate for porewater CH₄ per hour; Eq. 10, Methods) and system-level filter efficiency (i.e., derived from streambed to stream water CH₄ ratio Eq. 11, Methods) remained fixed. Replication of this outcome across distinct regions suggests that the relative responses of production and oxidation are likely to be general features of freshwater CH₄ cycling, even if absolute rates differ. For example, while significant *amounts* of CH₄ can be oxidised in the stratified water column of lakes and the turbid waters of large sluggish rivers and estuaries^{10,11} we contend the *relative* response of CH₄ oxidation to CH₄ production would be conserved.

Conclusion

Taken together, these considerations support the generality of our central conclusion: under warming, CH₄ production increases at a rate that CH₄ oxidation can match but not exceed, leaving system-level filter efficiency fixed and emissions rising. While the previous datasets provided here demonstrate conserved temperature sensitivities for emissions and production across ecosystems, our natural experiment shows parallel relationships at multiple levels of organisation — from methanogen and methanotroph abundance, to production and oxidation

potentials, through to emissions. This consistency across scales and across multiple regions spanning the Northern Hemisphere strongly suggests that the fixed filter efficiency we observed in streams in response to warming is likely to be a general property of freshwater CH₄ cycling.

Supplementary Fig. 4 | The degree of CH₄ over-saturation in stream water increased along the natural warming gradient ($n=148$ for 51 streams). The degree of CH₄ saturation is the ratio of the measured CH₄ concentration to the concentration at atmospheric equilibration at *in situ* stream temperature ($C_{\text{measured}}/C_{\text{saturation}} \times 100$ %, see equation [1] in the main text). Like streams worldwide that are recognised as sources of CH₄ to the atmosphere³, all the high-latitude streams here were over-saturated in CH₄ and the overall average degree of over-saturation increased with a temperature sensitivity of 0.53 eV (i.e., activation energy, 95% CI: 0.10 to 0.97 eV) along our natural temperature gradient from 1°C to 36°C. Solid line and shaded areas are posterior median and 95% credible intervals, respectively, both extracted from a hierarchical Bayesian linear mixed model.



Supplementary Table 1 | Current global CH₄ emissions and estimated increases with 2.5°C of warming under SSP2-4.5 for either a fixed or optimum CH₄ filter scenario.

	Scenarios		
	Current scenario	2.5°C-fixed scenario	2.5°C-optimum scenario
CH₄ production (Tg per year)	1437	2003	2003
CH₄ filter (%)	70	70	78
CH₄ emission (Tg per year)	431	601	431

The CH₄ filter oxidises the majority (typically 70% to 90%) of CH₄ produced in anoxic sediments back to CO₂ before emission to the atmosphere. The current global rate of CH₄ emissions from freshwater ecosystems is estimated to be 431 Tg CH₄ per year¹² and a conservative estimate of total CH₄ production would, accordingly, be 1437 Tg per year (i.e., $431/(100\%-70\%)=1437$, Fig. 1A – current scenario). All 1437 Tg produced per year could potentially be emitted to the atmosphere without the CH₄ filter. Under a future warming scenario of 2.5°C (projected for 2100, SSP2-4.5)¹³, and with the recognised temperature sensitivity for methanogenesis of 0.96 eV⁴, CH₄ production will increase by 1.4-fold and so will emissions if the CH₄ filter remains fixed at the same 70% efficiency (Fig. 1A – fixed scenario). In comparison, if the efficiency of the CH₄ filter increases disproportionately to 78% i.e., under the optimum scenario, emissions will be constrained at their current level of 431 Tg per year ($100\%-(431/2003) \times 100\%=78\%$) (Fig. 1A – optimum scenario).

Supplementary Table 2 | Idealised complete mineralisation of glucose to equimolar amounts of CO₂ and CH₄ (reaction 4) through a coupling of fermentation (reaction 1) to the hydrogenotrophic (reaction 2) and acetoclastic (reaction 3) pathways of methanogenesis, after^{6,14}. Note that the idealised 1:1 ratio for CO₂ to CH₄ production (reaction 4) can only be realised if all of the fermentation products (2 moles of CH₃COOH, 1 CO₂ and 4 moles of H₂) are subsequently used in methanogenesis, which seldom appears to be the case due to inefficient substrate use⁶. In addition, methylotrophic methanogenesis produces more CH₄ than CO₂ at a ratio of 3:1 (reaction 5, here we use methanol as a representative substrate for methylotrophic methanogenesis) but typically contributes only a minor portion of CH₄ production (< 5%) in freshwater sediments^{15,16}. Furthermore, the proportion of methylotrophic methanogens in freshwater sediments is typically small (<10%, see refs^{17–20} as examples) which agrees with what we found here with the methylotrophic methanogens constituting ~9% of the methanogen sequences in our streambeds (see Supplementary Figure 3). Note, the hydrogen-dependent methylotrophs accounted for an even smaller proportion of the methylotrophs (12.4% of 9%) and, therefore, were not likely to influence the measured increase in CH₄:CO₂.

Reaction	Stoichiometry	Metabolism
1	$C_6H_{12}O_6 + 2H_2O \rightarrow 2CH_3COOH + 2CO_2 + 4H_2$	Fermentation
2	$4H_2 + CO_2 \rightarrow 2H_2O + CH_4$	Hydrogenotrophic
3	$2CH_3COOH \rightarrow 2CO_2 + 2CH_4$	Acetoclastic
4	$C_6H_{12}O_6 \rightarrow 3CH_4 + 3CO_2$ (1:1 ratio)	Sum of 1 to 3
5	$4CH_3OH \rightarrow 3CH_4 + 1CO_2 + 2H_2O$ (3:1 ratio)	Methylotrophic

Supplementary Table 3 | Hydrophysical characteristics for the streams in the five high-latitude regions. Data are presented as median, first (Q1) and third (Q3) quartiles.

Region	Hydrophysical characteristics Median (Q1-Q3)			
	Width (m)	Depth (m)	Flow (m s ⁻¹)	<i>k</i> _{O₂, 20°C} (cm h ⁻¹)
Alaska (Manley Hot Springs)	1.0 (0.71-1.5)	0.2 (0.13-0.46)	0.24 (0.13-0.43)	33.6 (15.4-50.0)
Greenland (Qeqertarsuaq/ Disko Island)	0.44 (0.29-0.68)	0.1 (0.05-0.14)	0.33 (0.06-0.69)	24.1 (20.4-31.5)
Iceland (Hengill Valley)	0.87 (0.63-1.5)	0.09 (0.07-0.11)	0.28 (0.17-0.45)	72.2 (50.6-112)
Kamchatka ^{††} (Verkhne-Paratunskiye thermal springs)	0.58 (0.45-0.83)	0.04 (0.03-0.054)	0.37 (0.16-0.41)	125 (33.9-169)
Svalbard (North-Western Spitsbergen National Park)	0.48 (0.3-0.61)	0.06 (0.04-0.08)	0.13 (0.06-0.16)	80.6 (38.4-84.0)

Supplementary Table 4 | Chemical characteristics for the streams in the five high-latitude regions. Data are presented as median, first (Q1) and third (Q3) quartiles.

Region	Chemical characteristics of surface stream water Median (Q1-Q3)					Chemical characteristics of sediment porewater ^{†††} Median (Q1-Q3)	
	pH	TIN [†] ($\mu\text{mol L}^{-1}$)	SRP [†] ($\mu\text{mol L}^{-1}$)	Dissolved CH ₄ (nmol L^{-1})	Dissolved O ₂ ($\mu\text{mol L}^{-1}$)	Dissolved CH ₄ (nmol L^{-1})	Dissolved O ₂ ($\mu\text{mol L}^{-1}$)
Alaska (Manley Hot Springs)	7.6 (7.4-7.8)	2.2 (2.1-2.5)	0.93 (0.48-2.0)	174 (87-279)	325 (261-347)	155 (105-2670)	238 (154-317)
Greenland (Qeqertarsuaq/ Disko Island)	8.4 (7.8-10)	1.1 (0.8-1.6)	0.83 (0.54-0.96)	31 (18-68)	368 (268-399)	540 (95-4630)	250 (172-349)
Iceland (Hengill Valley)	8.1 (7.6-8.2)	0.8 (0.6-0.9)	1.1 (0.82-1.3)	41 (29-65)	302 (272-333)	114 (93-148)	256 (187-313)
Kamchatka ^{††} (Verkhne-Paratunskiye thermal springs)	7.5 (7.3-7.6)	5.7 (4.3-6.7)	4.2 (2.8-4.6)	35 (28-38)	330 (277-354)	144 (126-384)	265 (236-311)
Svalbard (North-Western Spitsbergen National Park)	7.9 (7.3-8.5)	4.4 (2.8-15.5)	1.3 (0.68-1.4)	43 (35-47)	330 (284-385)	NA	NA

[†]Total inorganic nitrogen (TIN) is the sum of NO₃⁻, NO₂⁻, NH₄⁺ and SRP is soluble reactive phosphorus (see Supplementary Methods). See Supplementary Figure 2 for a comparison with streams across continental Europe.

^{††}While Kamchatka is at a lower latitude than the other four regions, its snow-cover, stream temperature and remoteness sustain a similar climate.

^{†††}Porewater collected from 2 to 10 cm depth. Porewater probes could not be deployed in Svalbard, therefore no porewater CH₄ concentrations could be determined in this region.

Supplementary Table 5 | Parameter estimates to characterize the temperature sensitivity in methane-related processes. Mean parameter estimates, 95% credible intervals for lower (2.5%) and upper (97.5%) bound, effective sample size (Eff), and the Gelman-Rubin statistic (\hat{R}), were obtained using a Bayesian hierarchical model. See Methods for parameter notation and model fitting approach. Overall region-level model fits are visually demonstrated in Extended Data Figure 5.

(5a) For CH₄ emission:

	Parameter	Mean	2.5%	97.5%	Eff	\hat{R}
Regression coefficients	α	-0.04	-0.54	0.45	2559	1.00
	β	0.58	0.25	0.93	3361	1.00
Region-level parameters	$\sigma(a_{0j})$	0.14	0.00	0.48	3955	1.00
	$\sigma(a_{1j})$	0.20	0.01	0.54	1985	1.00
	$Cor(a_{0j}, a_{1j})$	0.06	-0.79	0.84	4882	1.00
Stream-level parameters	$\sigma(b_{0jk})$	1.09	0.84	1.40	2876	1.00
	$\sigma(b_{1jk})$	0.14	0.00	0.45	1547	1.00
	$Cor(b_{0jk}, b_{1jk})$	0.25	-0.70	0.91	4435	1.00
Distributional parameter	σ	0.80	0.70	0.93	5048	1.00

(5b) For CH₄ production:

	Parameter	Mean	2.5%	97.5%	Eff	\hat{R}
Regression coefficients	α	-4.34	-5.02	-3.46	3050	1.00
	β	0.73	0.31	1.13	4353	1.00
Region-level parameters	$\sigma(a_{0j})$	0.53	0.03	1.17	1689	1.00
	$\sigma(a_{1j})$	0.14	0.00	0.48	4261	1.00
	$Cor(a_{0j}, a_{1j})$	-0.01	-0.81	0.80	7943	1.00
Stream-level parameters	$\sigma(b_{0jk})$	0.62	0.02	1.24	863	1.00
	$\sigma(b_{1jk})$	0.19	0.01	0.63	3190	1.00
	$Cor(b_{0jk}, b_{1jk})$	0.12	-0.74	0.85	6252	1.00
Distributional parameter	σ	1.34	1.06	1.70	1811	1.00

(5c) For CH₄ to CO₂ production ratio:

	Parameter	Mean	2.5%	97.5%	Eff	\hat{R}
Regression coefficients	α	-3.50	-5.19	-1.62	3748	1.00

	β	1.15	0.55	1.73	9701	1.00
Region-level parameters	$\sigma(a_{0j})$	2.02	1.39	2.87	5662	1.00
	$\sigma(a_{1j})$	0.16	0.00	0.57	6262	1.00
	$Cor(a_{0j}, a_{1j})$	-0.04	-0.82	0.80	10883	1.00
Stream-level parameters	$\sigma(b_{0jk})$	0.18	0.00	0.62	6288	1.00
	$\sigma(b_{1jk})$	0.16	0.00	0.56	7096	1.00
	$Cor(b_{0jk}, b_{1jk})$	0.00	-0.81	0.81	12570	1.00
Distributional parameter	σ	2.03	1.70	2.43	9513	1.00

(5d) For CH₄ oxidation:

	Parameter	Mean	2.5%	97.5%	Eff	\hat{R}
Regression coefficients	α	-0.09	-0.99	0.85	3850	1.00
	β	0.69	0.23	1.13	5321	1.00
Region-level parameters	$\sigma(a_{0j})$	0.79	0.09	1.48	1759	1.00
	$\sigma(a_{1j})$	0.17	0.01	0.58	5404	1.00
Stream-level parameters	$\sigma(b_{0jk})$	1.35	0.88	1.91	2013	1.00
Distributional parameter	σ	1.32	1.09	1.62	4339	1.00

(5e) For *mcrA* abundance:

	Parameter	Mean	2.5%	97.5%	Eff	\hat{R}
Regression coefficients	α	8.04	7.33	8.75	3470	1.00
	β	0.41	0.05	0.77	3704	1.00
Region-level parameters	$\sigma(a_{0j})$	0.64	0.20	1.18	2113	1.00
	$\sigma(a_{1j})$	0.15	0.00	0.50	3946	1.00
	$Cor(a_{0j}, a_{1j})$	-0.05	-0.81	0.77	8727	1.00
Stream-level parameters	$\sigma(b_{0jk})$	0.96	0.72	1.26	1829	1.00
	$\sigma(b_{1jk})$	0.17	0.01	0.57	1504	1.00
	$Cor(b_{0jk}, b_{1jk})$	0.00	-0.77	0.77	8087	1.00
Distributional parameter	Shape	2.53	1.81	3.36	6399	1.00
	z_i	0.27	0.21	0.34	14510	1.00

(5f) For *pmoA* abundance:

	Parameter	Mean	2.5%	97.5%	Eff	\hat{R}
--	-----------	------	------	-------	-----	-----------

Regression coefficients	α	7.97	7.50	8.46	2844	1.00
	β	0.51	0.17	0.84	2958	1.00
Region-level parameters	$\sigma(a_{0j})$	0.31	0.01	0.79	1186	1.00
	$\sigma(a_{1j})$	0.13	0.00	0.46	3115	1.00
Stream-level parameters	$\sigma(b_{0jk})$	0.92	0.70	1.18	2427	1.00
Distributional parameter	Shape	1.56	1.18	2.00	4969	1.00
	z_i	0.11	0.06	0.16	9895	1.00

Supplementary Table 6 | Subset of sample DNA concentrations quantified in extracts used as templates for downstream molecular work as evidence of the low biomass within sediment, ordered from highest to lowest.

Sample ID	DNA concentration (ng/μL)	Sample ID	DNA concentration (ng/μL)	Sample ID	DNA concentration (ng/μL)	Sample ID	DNA concentration (ng/μL)	Sample ID	DNA concentration (ng/μL)
B8	15.6	51	3.4	11	1.1	HD	0.4	34	<0.1
98	12.1	92	3.4	5	1.1	37	0.4	89	<0.1
87	11.3	32	3.4	30	1.0	59	0.3	101	<0.1
5.3	10.8	61	3.3	73	1.0	6	0.3	46	<0.1
B2	9.2	63	3.1	72	1.0	70	0.3	90	<0.1
108	7.3	50	2.9	17	0.9	A5	0.3	48	<0.1
54	7.5	93	2.9	100	0.8	A1	0.2	79	<0.1
B9	7.4	74	2.8	C2	0.8	58	0.2	57	<0.1
97	7.0	52	2.8	49	0.7	44	0.3	13	<0.1
B6	6.6	HB	2.7	33	0.7	A4	0.2	99	<0.1
12	6.4	104	2.4	22	0.7	25	0.2	7	<0.1
21	6.2	81	2.2	A7	0.8	110	0.2	36	<0.1
5.1	6.0	18	2.3	29	0.7	B7	0.2	35	<0.1
43	6.0	41	2.2	31	0.7	C7	0.2		
28	5.3	8	2.1	47	0.6	27	0.2		
85	5.0	B10	2.1	91	0.6	66	0.1		
83	4.7	19	2.0	38	0.6	HA	0.1		
20	4.9	53	1.9	14	0.3	88	0.1		
94	4.5	95	1.9	105	0.5	102	0.1		

Supplementary Table 7 | Parameter estimates to evaluate changes in community diversity and community compositional changes along the natural warming gradient. Mean parameter estimates, 95% credible intervals for lower (2.5%) and upper (97.5%) bound, effective sample size (Eff.), and the Gelman-Rubin statistic (\hat{R}), were obtained using a Bayesian hierarchical model. See Methods for parameter notation and model fitting approach.

Prior to model fitting, the NGS reads of *mcrA* sequences were rarefied to 1,000 reads per sample and the proportion of methanogen families (i.e., *Methanobacteriaceae*, *Methanocellaceae*, *Methanoregulaceae*, *Methanotrochaceae* and Methylophs, see Extended Data Figure 6) in each sample calculated as reads of family per 1,000 reads per sample. For *pmoA* sequences, the NGS reads were rarefied to 1,006 reads per sample (the minimum sample size of the *pmoA* library) and the proportion of methanotroph types (i.e., type I and type II, see Extended Data Figure 7) in each sample calculated as reads of type per 1,006 reads per sample. The methanogen or methanotroph communities were first assessed using Shannon index (**Tables 7a** and **7b**), followed by an analysis of the relative abundance of methanogen families and methanotroph types (**Table 7cs** and **7d**).

(7a) For Shannon index in *mcrA* community:

	Parameter	Mean	2.5%	97.5%	Eff.	\hat{R}
Regression coefficients	α	1.07	0.88	1.25	2839	1.00
	β	0.01	-0.18	0.18	2659	1.00
	$\sigma(a_{0j})$	0.13	0.00	0.36	1924	1.00
Region-level parameters	$\sigma(a_{1j})$	0.10	0.00	0.32	2496	1.00
	$Cor(a_{0j}, a_{1j})$	-0.10	-0.84	0.75	6086	1.00
	$\sigma(b_{0jk})$	0.27	0.16	0.38	2724	1.00
Stream-level parameters	$\sigma(b_{1jk})$	0.06	0.00	0.20	2003	1.00
	$Cor(b_{0jk}, b_{1jk})$	0.03	-0.78	0.82	5953	1.00
Distributional parameter	σ	0.32	0.28	0.37	5197	1.00

(7b) For Shannon index in *pmoA* community:

	Parameter	Mean	2.5%	97.5%	Eff.	\hat{R}
Regression coefficients	α	0.31	0.15	0.48	4061	1.00
	β	-0.04	-0.14	0.06	4410	1.00

	$\sigma(a_{0j})$	0.16	0.12	0.21	3745	1.00
Region-level parameters	$\sigma(a_{1j})$	0.04	0.00	0.12	1432	1.00
	$Cor(a_{0j}, a_{1j})$	0.17	-0.72	0.86	6255	1.00
	$\sigma(b_{0jk})$	0.16	0.06	0.36	3895	1.00
Stream-level parameters	$\sigma(b_{1jk})$	0.07	0.00	0.21	2577	1.00
	$Cor(b_{0jk}, b_{1jk})$	-0.02	-0.79	0.76	9697	1.00
Distributional parameter	σ	0.16	0.15	0.18	9191	1.00

(7c) For compositional changes in *mcrA* community:

	Parameter	Mean	2.5%	97.5%	Eff.	\widehat{R}
	α	0.31	0.25	0.37	3490	1.00
	β_1	0.03	-0.02	0.07	3641	1.00
	$\gamma_{g=\text{Methanobacteriaceae}}$	-0.04	-0.11	0.03	6097	1.00
	$\gamma_{g=\text{Methanoregulaceae}}$	0.31	0.25	0.38	6081	1.00
	$\gamma_{g=\text{Methanotrichaceae}}$	0.17	0.10	0.23	5796	1.00
Regression coefficients	$\gamma_{g=\text{Methyloph}}$	-0.03	-0.10	0.23	5796	1.00
	$\delta_{g=\text{Methanobacteriaceae}}$	0.03	-0.04	0.10	4706	1.00
	$\delta_{g=\text{Methanoregulaceae}}$	-0.13	-0.20	-0.06	4670	1.00
	$\delta_{g=\text{Methanotrichaceae}}$	0.01	-0.06	0.08	5057	1.00
	$\delta_{g=\text{Methyloph}}$	-0.04	-0.11	0.03	4799	1.00
Region-level parameters	$\sigma(a_{0j})$	0.03	0.00	0.09	2436	1.00
Stream-level parameters	$\sigma(b_{0jk})$	0.01	0.00	0.03	6022	1.00
Distributional parameter	σ	0.27	0.26	0.29	14589	1.00

Note that the terms δ_g are the category-specific temperature interaction effects relative to the baseline (β_1 , corresponding to *Methanocellaceae*; see Eq.21 in the Methods). The slopes (β) and their credible intervals shown in Fig.3B and 3C correspond to the overall estimated slopes for each taxonomic category, derived from the posterior draws. The posterior probabilities for the slopes being positive or negative were assessed using one-sided hypothesis testing and are measures of Bayesian evidence supporting directional effects.

(7d) For compositional changes in *pmoA* community:

	Parameter	Mean	2.5%	97.5%	Eff.	\hat{R}
Regression coefficients	α	0.51	0.44	0.57	6271	1.00
	β_1	-0.06	-0.12	0.00	6161	1.00
	$\gamma_{g=\text{type II}}$	0.56	0.48	0.65	7881	1.00
	$\delta_{g=\text{type II}}$	0.12	0.04	0.21	6066	1.00
Region-level parameters	$\sigma(a_{0j})$	0.03	0.00	0.09	4016	1.00
Stream-level parameters	$\sigma(b_{0jk})$	0.02	0.00	0.05	5830	1.00
Distributional parameter	σ	0.42	0.40	0.45	10812	1.00

Note that the terms δ_g is the temperature interactions of type II methanotroph relative to baseline (β_1 , corresponding to type I methanotroph, see Eq.21 in the Methods). The slopes (β) and their credible intervals shown in Fig.3E and 3F correspond to the overall estimated slopes for each methanotroph type, derived from posterior draws. The posterior probabilities for the slopes being positive or negative were assessed using one-sided hypothesis testing and are measures of Bayesian evidence supporting directional effects.

Supplementary Table 8 | Parameter estimates to evaluate process-level CH₄ oxidation efficiency and system-level CH₄ filter efficiency. Mean parameter estimates, 95% credible intervals for lower (2.5%) and upper (97.5%) bound, effective sample size (Eff.), and the Gelman-Rubin statistic (\hat{R}), were obtained using a Bayesian hierarchical model. See Methods for parameter notation and model fitting approach.

(8a) For process-level CH₄ oxidation efficiency:

	Parameter	Mean	2.5%	97.5%	Eff.	\hat{R}
Regression coefficients	α	-0.10	-1.33	1.11	6570	1.00
	β	0.25	-0.79	1.30	8210	1.00
	$\sigma(a_{0j})$	0.99	0.25	1.72	2642	1.00
Region-level parameters	$\sigma(a_{1j})$	0.23	0.01	0.85	7618	1.00
	$Cor(a_{0j}, a_{1j})$	0.12	-0.75	0.86	15871	1.00
	$\sigma(b_{0jk})$	1.12	0.24	1.79	1717	1.00
Stream-level parameters	$\sigma(b_{1jk})$	0.22	0.01	0.85	7752	1.00
	$Cor(b_{0jk}, b_{1jk})$	0.07	-0.77	0.83	15615	1.00
Distributional parameter	σ	1.52	1.21	1.98	2824	1.00

Note that the term β is the effect of warm streams relative to cold streams α (see Eq. 23 in the Methods). The process-level CH₄ oxidation efficiency in the cold and warm streams and their credible intervals reported in Fig.4C in the main text are estimated from posterior draws.

(8b) For system-level CH₄ filter efficiency:

	Parameter	Mean	2.5%	97.5%	Eff.	\hat{R}
Regression coefficients	α	1.09	0.47	1.71	3065	1.00
	β	0.02	-0.84	0.87	3479	1.00
	$\sigma(a_{0j})$	0.21	0.01	0.67	2666	1.00
Region-level parameters	$\sigma(a_{1j})$	0.22	0.01	0.81	4093	1.00
	$Cor(a_{0j}, a_{1j})$	0.00	-0.81	0.81	10471	1.00
	$\sigma(b_{0jk})$	1.01	0.67	1.41	2963	1.00
Stream-level parameters	$\sigma(b_{1jk})$	0.19	0.01	0.69	3556	1.00
	$Cor(b_{0jk}, b_{1jk})$	0.03	-0.77	0.82	11022	1.00
Distributional parameter	φ	11.50	7.11	16.86	4508	1.00

Note that, as the system-level CH₄ filter efficiency is a continuous proportion bounded between 0 and 1, we fitted a beta regression model with logit link (see Eq.24 in the Methods). Therefore, the numbers reported here are on the logit-transformed scale. The efficiency estimates and credible intervals presented in Fig. 4D were derived by applying the inverse logit transformation to posterior draws. For example, α - the intercept representing the process-level CH₄ oxidation efficiency for cold streams – is 1.09 on the logit scale. Applying the inverse logit transformation: $\frac{e^{1.09}}{1+e^{1.09}}=0.75$, i.e., corresponds to 75% efficiency. Similarly, β is the effect of warm streams relative to cold streams on the logit scale; combined with the intercept, this gives:

$$\frac{e^{(1.09+0.02)}}{1+e^{(1.09+0.02)}}=0.75, \text{ i.e., 75\% efficiency for warm streams.}$$

Supplementary Table 9 | Primer sets for qPCR and NGS.

A, Primer sets used in both qPCR and NGS library preparation to target methanogenic Archaea (*mcrA*) and methanotrophic Bacteria (*pmoA*) with both primer sets containing the same locus specific regions. The primer sets used for NGS include Illumina overhang adapters for binding to the Illumina flow cell²³.

Target gene	Primer name	Primer sequence (5'-3')
<i>mcrA</i> (Methyl coenzyme M reductase)	mlas-mod ^{†24,25}	5'-GGYGGTGTMGDDTTACMCARTA-3'
	mcrA-rev ²⁵	5'-CGTTCATBGCCTAGTTVGGRTAGT-3'
<i>pmoA</i> (Particulate methane monooxygenase)	A189 ²⁶	5'-GGNGACTGGGACTTCTGG-3'
	A650 ²⁷	5'-ACGTCCTTACCGAAGGT-3'

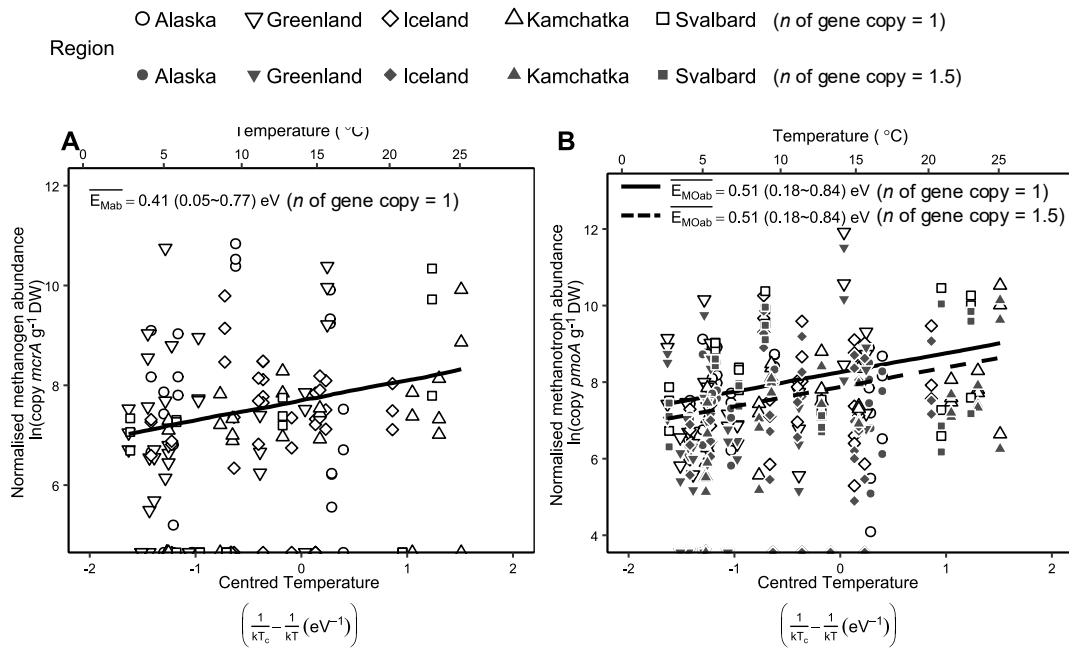
[†] *mlas-mod* is only 1 bp different from original *mlas* forward primer²⁵

Use of qPCR to estimate methanogen and methanotroph abundance. Steinberg and Regan (2009)²⁸ examined the complete genomes of 19 methanogens submitted to GenBank and found only one copy of *mcrA* in all 19 and we could find no evidence of multiple copies of *mcrA* in the 356 papers citing them since. Further, while members of the *Methanococcales* and *Methanobacteriales* do also contain a copy of the *mrtA* variant of *mcrA* we could find no evidence from all of our sequences to indicate any amplification of *mrtA*, nor in the literature that used the same primer pair as we did – see Emilson *et al.* 2018 (ref.²⁹); Zhang *et al.* 2020 (ref.³⁰) as examples. In contrast, it is recognised that the genomes of some methanotrophs do contain multiple copies of *pmoA* (**B**, below). We searched in KEGG, the genome database and individual published species descriptions for *pmoA* copy number (below and see literature list provided as a separate supporting file) and found copy numbers in type I methanotrophs to be like those for type II methanotrophs, with an overall average of 1.5 which is close to the 1.62 reported previously³¹.

Genus	Type	Species	Strains	Range of copy number	Average copy number
<i>Methylomonas</i>	Type I	27	31	1-3	1.6
<i>Methylobacter</i>	Type I	7	10	1-2	1.8
<i>Methylococcus</i>	Type I	3	3	2	2
<i>Methylocaldum</i>	Type I	2	2	2	2
<i>Methylobacterium</i>	Type I	6	7	1-2	1.3

<i>Methylosarcina</i>	Type I	1	2	1	1
Average across type I genus					1.6
<i>Methylosinus</i>	Type II	1	1	1	1
<i>Methylocystis</i>	Type II	9	9	1-3	2.2
<i>Methylocapsa</i>	Type II	3	1	1	1
Average across type II genus					1.4
Average across types					1.5

As *pmoA* copy number was comparable between the type I and type II methanotrophs we used the overall average of 1.5 across the two types to correct the increase in methanotroph abundance in response to warming presented in Fig. 4B in the main text and below. Note that while the correction to *pmoA* copy number (panel B, below) reduced the average estimate of methanotroph abundance (i.e., the intercept at T_c) the response to warming i.e., their temperature sensitivity (slope) remained the same at 0.51 eV.



References

1. Kirkwood, D. Nutrients: Practical notes on their determination in sea water. *ICES Tech. Mar. Environ. Sci.* **17**, 25 (1996).
2. Si, Y. *et al.* Direct biological fixation provides a freshwater sink for N₂O. *Nat. Commun.* **14**, 6775 (2023).
3. Chang, K.-Y., Riley, W. J., Crill, P. M., Grant, R. F. & Saleska, S. R. Hysteretic temperature sensitivity of wetland CH₄ fluxes explained by substrate availability and microbial activity. *Biogeosciences* **17**, 5849–5860 (2020).
4. Yvon-Durocher, G. *et al.* Methane fluxes show consistent temperature dependence across microbial to ecosystem scales. *Nature* **507**, 488–91 (2014).
5. Zhu, Y. *et al.* Separating natural from human enhanced methane emissions in headwater streams. *Nat. Commun.* **13**, 3810 (2022).
6. Zhu, Y., Purdy, K. J., Martínez Rodríguez, A. & Trimmer, M. A rationale for higher ratios of CH₄ to CO₂ production in warmer anoxic freshwater sediments and soils. *Limnol. Oceanogr. Lett.* **8**, 398–405 (2023).
7. Rovelli, L. *et al.* Contrasting biophysical controls on carbon dioxide and methane outgassing from streams. *J. Geophys. Res. Biogeosciences* **1**, 2–31 (2021).
8. Langenegger, T., Vachon, D., Donis, D. & McGinnis, D. F. What the bubble knows: Lake methane dynamics revealed by sediment gas bubble composition. *Limnol. Oceanogr.* **64**, 1526–1544 (2019).
9. Zhu, Y. *et al.* Disproportionate increase in freshwater methane emissions induced by experimental warming. *Nat. Clim. Change* **10**, 685–690 (2020).
10. Patel, L., Singh, R., Gowd, S. C. & Thottathil, S. D. Environmental determinants of aerobic methane oxidation in a tropical river network. *Water Res.* **265**, 122257 (2024).

11. Matoušů, A., Osudar, R., Šimek, K. & Bussmann, I. Methane distribution and methane oxidation in the water column of the Elbe estuary, Germany. *Aquat. Sci.* **79**, 443–458 (2017).
12. Rosentreter, J. A. *et al.* Half of global methane emissions come from highly variable aquatic ecosystem sources. *Nat. Geosci.* **14**, 225–230 (2021).
13. Hausfather, Z. & Peters, G. P. Emissions – the ‘business as usual’ story is misleading. *Nature* **577**, 618–620 (2020).
14. Conrad, R. Contribution of hydrogen to methane production and control of hydrogen concentrations in methanogenic soils and sediments. *FEMS Microbiol. Ecol.* **28**, 193–202 (1999).
15. Conrad, R. & Claus, P. Contribution of methanol to the production of methane and its ¹³C-isotopic signature in anoxic rice field soil. *Biogeochemistry* **73**, 381–393 (2005).
16. Lovley, D. R. & Klug, M. J. Methanogenesis from methanol and methylamines and acetogenesis from hydrogen and carbon dioxide in the sediments of a eutrophic lake. *Appl. Environ. Microbiol.* **45**, 1310–1315 (1983).
17. Rasmussen, A. N., Tolar, B. B., Bargar, J. R., Boye, K. & Francis, C. A. Diverse and unconventional methanogens, methanotrophs, and methylotrophs in metagenome-assembled genomes from subsurface sediments of the Slate River floodplain, Crested Butte, CO, USA. *mSystems* **9**, e00314-24 (2024).
18. Narrowe, A. B. *et al.* Uncovering the Diversity and Activity of Methylotrophic Methanogens in Freshwater Wetland Soils. *mSystems* **4**, 10.1128/msystems.00320-19 (2019).

19. Söllinger, A. *et al.* Phylogenetic and genomic analysis of *Methanomassiliicoccales* in wetlands and animal intestinal tracts reveals clade-specific habitat preferences. *FEMS Microbiol. Ecol.* **92**, fiv149 (2016).
20. Ellenbogen, J. B. *et al.* Methylotrophy in the Mire: direct and indirect routes for methane production in thawing permafrost. *mSystems* **9**, e00698-23 (2024).
21. Brooks, M. E. *et al.* glmmTMB balances speed and flexibility among packages for zero-inflated generalized linear mixed modeling. *R J.* **9**, 378–400 (2017).
22. Lenth, R. emmeans: Estimated Marginal Means, aka Least-Squares Means. (2019).
23. Illumina. 16S Metagenomic Sequencing Library. *Illumina.com* 1–28 (2013).
24. Angel, R., Claus, P. & Conrad, R. Methanogenic archaea are globally ubiquitous in aerated soils and become active under wet anoxic conditions. *Isme J.* **6**, 847 (2011).
25. Steinberg, L. M. & Regan, J. M. Phylogenetic comparison of the methanogenic communities from an acidic, oligotrophic fen and an anaerobic digester treating municipal wastewater sludge. *Appl. Environ. Microbiol.* **74**, 6663–6671 (2008).
26. Holmes, A. J., Costello, A., Lidstrom, M. E. & Murrell, J. C. Evidence that participate methane monooxygenase and ammonia monooxygenase may be evolutionarily related. *FEMS Microbiol. Lett.* **132**, 203–208 (1995).
27. Bourne, D. G., McDonald, I. R. & Murrell, J. C. Comparison of *pmoA* PCR Primer Sets as Tools for Investigating Methanotroph Diversity in Three Danish Soils. *Appl. Environ. Microbiol.* **67**, 3802–3809 (2001).
28. Steinberg, L. M. & Regan, J. M. *mcrA*-targeted real-time quantitative PCR method to examine methanogen communities. *Appl. Environ. Microbiol.* **75**, 4435–4442 (2009).

29. Emilson, E. J. S. *et al.* Climate-driven shifts in sediment chemistry enhance methane production in northern lakes. *Nat. Commun.* **9**, 1801 (2018).
30. Zhang, C.-J., Pan, J., Liu, Y., Duan, C.-H. & Li, M. Genomic and transcriptomic insights into methanogenesis potential of novel methanogens from mangrove sediments. *Microbiome* **8**, 94 (2020).
31. Nijman, T. P. A. *et al.* Warming and eutrophication interactively drive changes in the methane-oxidizing community of shallow lakes. *ISME Commun.* **1**, 32 (2021).